Micro- and Nanotechnology: Materials, Processes, Packaging, and Systems IV
edited by Jung-Chih Chiao, Alex J. Hariz, David V. Thiel, Changyi Yang, Proc. of SPIE
Vol. 7269, 72690I · © 2008 SPIE · CCC code: 0277-786X/08/$18 · doi: 10.1117/12.813893

An effective multiscale approach for deformation analyses of carbon nanotube-based nanoswitches

Y.T. Gu*, A. Tan and Prasad K.D.V. Yarlagadda
School of Engineering Systems, Queensland University of Technology,
GPO Box 2434, Brisbane, QLD 4001, Australia

ABSTRACT

This paper aims to develop an effective multiscale simulation technique for the deformation analysis of nanotube-based nanoswitches. In the multiscale simulation, the key material parameters, (e.g., Young's modulus and moment of inertia) are extracted from the MD simulation which can explore the atomic properties. Then, the switches are simplified to continuum structure which is discretized and simulated by the advanced RBF meshfree formulation. The system of equations is nonlinear because the nonlinear loading is calculated from coupled the electrostatic, the elastostatic, and the van der Waals energy domains. Besides the normal deformation analysis, the pull-in voltage characteristics of different nanoswitches based on the double-walled nanotubes are analyzed. Comparing with the results in the literature and from experiments, it has proven that the developed multiscale approach is accurate and efficient.

Keywords: NEMS, Nanotube; Multiscale; Molecular dynamics; Meshfree

1. INTRODUCTION

Due to the new development of science and technology, the size of devices is becoming smaller and smaller. Beyond the microelectromechanical systems (MEMS), recently, the nano-devices which are called nanoelectromechanical systems (NEMS) are attracting the researchers. In the family of NEMS, the nanoswitch is an important type of devices with broad applications and can be made based on carbon nanotubes which have excellent electronic, chemical and mechanical properties. Because of the small dimensional scale, experiments on nanoswitches are limited or even impossible for many cases and devices. Numerical modelling and simulations have therefore become important tools in analysis and design of NEMS especially of nanoswitches. Molecular dynamics (MD) is a powerful numerical simulation tool for the problems in nanoscales. There are several ways to describe an MD analysis, physically [1] or mathematically [2]. MD has been widely used in the simulation of nanotubes.

Let's firstly brief the development of multiscale modeling techniques. For many cases in advanced engineering and science, molecular dynamics and continuum-based theories are not applicable across the full range of scales. For molecular dynamics, the systems are usually too large to be analyzed; for continuum-based theories, the atomic behaviour of the systems is too small to be analyzed. Because of these intractable problems, there have been significant international efforts to develop multiscale theories to integrate the atomistic and continuum theories [3-5], especially crossing length scale, by applying an atomistic theory in a small length scale in which an accurate capture of atomic dynamics is crucial, and employing a continuum theory in large scales where deformation is smooth enough to make the theory applicable. This is the multiscale modelling technique, which is widely recognized as an essential part of computational science and engineering. Some research teams have embedded the intrinsic atomic properties of a solid in their continuum formulations. However, their theories are based on the assumption of homogeneous lattice deformation and are therefore unsuitable for solving problems with defects in atomic lattices, such as dislocations and phase changes. Some other teams have used a more flexible approach[6]. At each spatial scale, they apply the theories that are valid for that scale to attempt a smooth coupling of the data. However, there are critical problems associated with this approach, due to the lack of theoretically robust techniques to identify the transition region between the scales and to integrate the data. Clearly, the development of the multiscale simulation techniques is still at its infancy, and there are many technical problems remained.

In recent years, a group of advanced meshfree numerical techniques [7][8], have been developed and achieved remarkable progress for the continuum analysis. The meshfree methods using various weak-forms of the ordinary differential equations (ODEs) or the partial differential equations (PDEs) of the problems, e.g., the element-free Galerkin (EFG) method [9], the meshless local Petrov-Galerkin (MLPG) method [10], and the local radial point interpolation method (LRPIM) [8][11], have shown many distinguished advantages in the applications for engineering and sciences. In summary, the meshfree methods have the following distinguished advantages[7]:

* yuantong.gu@qut.edu.au; phone 61-7-31381009; fax 61-7-31381469

Micro- and Nanotechnology: Materials, Processes, Packaging, and Systems IV
edited by Jung-Chih Chiao, Alex J. Hariz, David V. Thiel, Changyi Yang, Proc. of SPIE
Vol. 7269, 72690I · © 2008 SPIE · CCC code: 0277-786X/08/$18 · doi: 10.1117/12.813893

- They do not use a mesh, so that the burden of mesh generation in FEM is overcome and a smooth atomic-continuum transition becomes possible.
- They are usually more accurate than FEM due to the use of higher order trial functions.
- They are capable of solving complex problems that are difficult for the conventional FEM to apply.

Because of these advantages, meshfree methods seem to have a good potential for multiscale analysis and have attracted the attention of the research community [5][12]. However, the topic is relatively new, and calls for a significant development.

Considering the properties of nanotube-based nanoswitches, this paper will develop an effective multiscale method for the characterizing the deformation of typical Nanoswitches whose key components are a double-walled carbon nanotube (DWNT) and a fixed ground plane. The reason that we call the newly developed technique as a "general multiscale" method is because both nanoscale technique, MD, and the continnum technique, meshfree method, are used at the same time. When a potential difference is created between the nanotube and the ground plane, electrostatic charges, which will lead to electrostatic force, are introduced. Meanwhile, elastostatic and van der Waals forces co-exist. Under an applied voltage, an equilibrium position of the tube is defined by the balance of the elastostatic, electrostatic and the van der Waals forces. To simulate these nanoswitches, an effective multiscale technique is developed based on the MD and a parameterized continuum model. The product of Young's modulus and moment of inertia of the DWNT will be determined by a molecular dynamics simulation with a linear deflection approximation. The switch will ten be simplified to a beam system, and the loading be calculated from three coupled energy domains: the electrostatic energy domain, the elastostatic energy domain, and the van der Waals energy domain. A meshfree formulation [7] will then be developed to discretize the domain of the switch to establish the non-linear equations for deformation analysis. The pull-in voltage characteristics of fixed-fixed and cantilever nanoswitches based on the DWNT are analyzed.

2. MATERIAL PARAMETERS FROM MD

This paper will deal with two typical nanoswitches[13], as shown in figures 1, whose key components are a double-walled carbon nanotube (DWNT) and a fixed ground plane. When a potential difference is created between the nanotube and the ground plane, electrostatic charges, which will lead to electrostatic force, are introduced. Meanwhile, elastostatic and van der Waals forces co-exist. Under an applied voltage, an equilibrium position of the tube is defined by the balance of the elastostatic, electrostatic and the van der Waals forces.

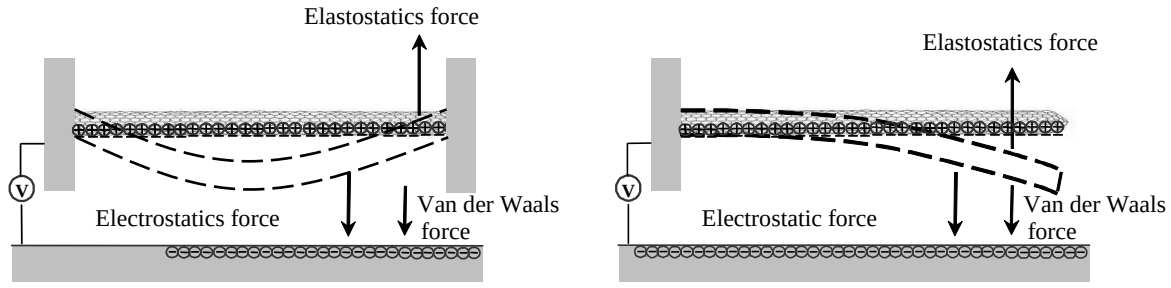

Fig. 1. fixed-fixed and cantilever nanoswitches based on DWNT

When the deflection of the nanotube is small and its cross-section shape change during bending is negligible, the nanotube in the switch can be simplified to a beam structure[14]. To use this beam continuum model, Young's modulus, *E*, and the moment of inertia, *I*, should be determined. There are many techniques to determine Young's modulus [15], but to date, there is no agreement about the exact value of the effective thickness, *h*, and *E* of a carbon nanotube. Some studies assumed that a nanotube was a solid cylinder, and the equivalent *h* and *E* are then calculated. Vodenitcharova and Zhang[15] pointed out that this assumption is incorrect because the tube is evidently not solid and continuous among atoms. Their model predicted that the equivalent thickness of a single-walled carbon nanotube should be 0.617 Å, which is 43.8% of the theoretical diameter of a carbon atom, and that the Young's modulus of this tube is 4.88Tpa. However, there is few study of equivalent thickness of a multi-walled carbon nanotube, which will be used to determine *E* and *I*.

Micro- and Nanotechnology: Materials, Processes, Packaging, and Systems IV
edited by Jung-Chih Chiao, Alex J. Hariz, David V. Thiel, Changyi Yang, Proc. of SPIE
Vol. 7269, 72690I · © 2008 SPIE · CCC code: 0277-786X/08/$18 · doi: 10.1117/12.813893

In this paper, the linear elasticity model for the DWNT is considered, and E and I are therefore constants. Hence, the linear deflection approximation, in which the peak deflection of the tube is considered as a linear function of the applied load, can be used to get the E and I together. The peak deflections for different loadings are firstly obtained by the MD simulation[16], as figure 2, and then using the classic beam theory to calculate EI. For example, for a cantilever or fixed-fixed tube, if the peak deflection is w_1 (obtained by MD simulation) when the force is f_1, and w_2 when the force is f_2, we can simply obtain EI:

$$EI = \frac{1}{2}\left(\frac{l^4}{8S_1} + \frac{l^4}{8S_2}\right) \quad \text{for a cantilever tube, and} \tag{1}$$

$$EI = \frac{1}{2}\left(\frac{l^4}{384S_1} + \frac{l^4}{384S_2}\right) \quad \text{for a fixed-fixed tube} \tag{2}$$

where l is the length of the tube, and S_1 and S_2 are the slopes of the MD load-deflection curve, i.e.,

$$S_1 = \frac{w_1}{f_1} \quad \text{and} \quad S_2 = \frac{w_2}{f_2} \tag{3}$$

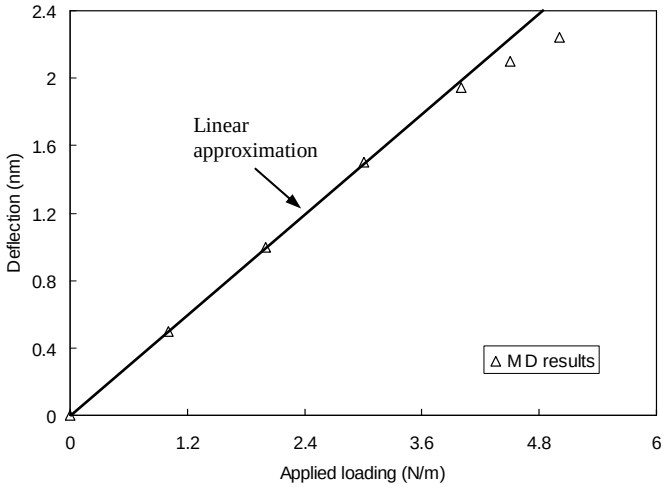

Fig. 2. Peak deflection versus applied force for a fixed–fixed DWNT

3. CONTINUNIM MESHFREE FORMULATION

When the deflection of the nanotube is small and its cross-section shape change during bending is negligible, the nanotube in the switch can be simplified to a beam structure. According to the continuum theory, the governing equation for the beam can be written as [14]

$$EI\frac{d^4w}{dx^4} = f \tag{4}$$

where w is the deflection of the nanotube, E is its Young's modulus, I is its moment of inertia, and f is the force per unit length on the tube. There are four boundary conditions, two at each end. The boundary conditions are given at the global boundary, Γ, as

for a fixed-fixed tube

$$\begin{aligned} w(0) &= 0, \quad \theta(0) = 0, \\ w(l) &= 0, \quad \theta(l) = 0\ ; \end{aligned} \tag{5}$$

Micro- and Nanotechnology: Materials, Processes, Packaging, and Systems IV
edited by Jung-Chih Chiao, Alex J. Hariz, David V. Thiel, Changyi Yang, Proc. of SPIE
Vol. 7269, 72690I · © 2008 SPIE · CCC code: 0277-786X/08/$18 · doi: 10.1117/12.813893

for a cantilever tube

$$\begin{aligned} w(0) = 0, \quad \theta(0) = 0, \\ M(l) = 0, \quad Q(l) = 0, \end{aligned} \tag{6}$$

where θ, M and Q denote the deflection slope, the bending moment and the shear force, respectively, and l is the length of the tube.

A local weak form of the differential equation (4), over a local domain Ω_q bounded by Γ_q, can be obtained using the local weighted residual method [7]

$$\int_{\Omega_q} \hat{w}(EI\frac{d^2w}{dx^2} - f)dx = 0 \tag{7}$$

where $\hat{w}$ is the weight function. The first term on the left hand side of equation (7) can be integrated by parts to become[11]

$$\int_{\Omega_q} (EI\hat{w}''w'' - \hat{w}f)\mathrm{d}x - \left[\bar{n}EI\hat{w}'w''\right]_{\Gamma_q} + \left[\bar{n}EI\hat{w}w'''\right]_{\Gamma_q} = 0 \tag{8}$$

where $\bar{n}$ is the unit outward normal to domain Ω_q.

An arbitrary shape quadrature domain can be used, such as a linear support domain for one-dimensional problems. It can be found that the boundary Γ_q for the support domain usually comprises five parts: the internal boundary Γ_{qi}, the boundaries Γ_{qw}, $\Gamma_{q\theta}$, Γ_{qM}, and Γ_{qQ}, over which the essential boundary conditions w, θ and natural boundary conditions M, Q are specified. The boundaries Γ_{qw} with Γ_{qQ} and $\Gamma_{q\theta}$ with Γ_{qM} are mutually disjoint. Imposing the natural (force) boundary condition, we obtain:

$$\begin{aligned} &\int_{\Omega_q} (EI\hat{w}''w'' - \hat{w}f)\mathrm{d}x - \left[\bar{n}\bar{M}\hat{w}'\right]_{\Gamma_{qM}} - \left[\bar{n}\bar{V}\hat{w}\right]_{\Gamma_{qQ}} - \left[\bar{n}EI\hat{w}'w''\right]_{\Gamma_{q\theta}} + \left[\bar{n}\hat{w}EIw'''\right]_{\Gamma_{qw}} \\ &- \left[\bar{n}\hat{w}'EIw''\right]_{\Gamma_{qi}} + \left[\bar{n}\hat{w}EIw'''\right]_{\Gamma_{qi}} = 0 \end{aligned} \tag{9}$$

If the value and the derivatives of the weight function $\hat{w}$ are taken to be zero at Γ_{qi}, the last two terms in equation (9) vanish.

The problem domain Ω is represented by properly scattered field nodes, and the Hermite point interpolation [7][11] is used to approximate the value of a point x

$$w(x) = \mathbf{\Phi}_w{}^{\mathrm{T}}(x)\mathbf{w} + \mathbf{\Phi}_\theta{}^{\mathrm{T}}(x)\boldsymbol{\theta} \tag{10}$$

where $\mathbf{w}$ and $\boldsymbol{\theta}$ denote the nodal deflections and slopes, respectively, and $\mathbf{\Phi}_w(x)$ and $\mathbf{\Phi}_\theta(x)$ are meshfree shape functions for deflection and slope, respectively. $\mathbf{\Phi}_w(x)$ and $\mathbf{\Phi}_\theta(x)$ will be discussed in Section 4.

As this local meshfree method is regarded as a weighted residual method, the weight function plays an important role in the performance of the method. It can be found that a weight function with the local property will yield better results, such as the quartic spline function. Following the idea of the Galerkin FEM, the weight function $\hat{w}$ can be taken as

$$\hat{w}(x_Q) = \mathbf{\Psi}_w{}^{\mathrm{T}}(x)\boldsymbol{\alpha} + \mathbf{\Psi}_\theta{}^{\mathrm{T}}(x)\boldsymbol{\beta} \tag{11}$$

where $\boldsymbol{\alpha}$ and $\boldsymbol{\beta}$ denote the fictitious nodal coefficients, $\mathbf{\Psi}_w$ and $\mathbf{\Psi}_\theta$ are constructed using meshfree shape functions. It should be noted that the support domain used to construct $\mathbf{\Psi}_w$ and $\mathbf{\Psi}_\theta$ can be independent of the support domain used to construct $\mathbf{\Phi}_w$ and $\mathbf{\Phi}_\theta$.

Substituting equations (10) and (11) into the local weak form equation (9) for all field nodes leads to the following discrete equations

$$\mathbf{K}\mathbf{w}^e = \mathbf{f} \tag{12}$$

It can be found that the above equation is nonlinear because that f is also the function of the deflection. Thus an iteration technique, the Newton-Raphson method, is required for its solution.

The total force in equation (4), f can be calculated as

Micro- and Nanotechnology: Materials, Processes, Packaging, and Systems IV
edited by Jung-Chih Chiao, Alex J. Hariz, David V. Thiel, Changyi Yang, Proc. of SPIE
Vol. 7269, 72690I · © 2008 SPIE · CCC code: 0277-786X/08/$18 · doi: 10.1117/12.813893

$$f = f_1 + f_2 \tag{13}$$

where f_1 is the electrostatic force per unit length and f_2 is van der Waals force. The electrostatic force can be computed by using a standard capacitance model [17], in which the nanotube is considered as a perfect cylindrical conductor. This implies that the potential is constant along the length of the tube. The capacitance per unit length for the cylindrical beam over a conductive ground plane is given by [18]. The electrostatic energy per unit length is given by

$$\Phi_{elec} = \frac{1}{2}C(r)V^2 = \frac{1}{2}V^2 \frac{\pi\varepsilon_0}{\log\left[1+g/r_1+\sqrt{(g/r_1+1)^2-1}\right]} \tag{14}$$

where ε_0 is the permittivity at vacuum, g is the gap between the nanotube and ground plane, and r_1 is the radius of the conductor (i.e. the exterior radius of the tube), V is the voltage applied. Therefore, the electrostatic force per unit length can be written as

$$f_1 = \frac{d\Phi_{elec}}{dr} = -\pi\varepsilon_0 V^2 \left\{ r_1 \left[g(g+2r_1)/r_1^2 \right]^{1/2} \log^2 \left\{ 1+g/r_1+\left[g(g+2r_1)/r_1^2 \right]^{1/2} \right\} \right\}^{-1} \tag{15}$$

The van der Waals force can be computed through the van der Waals energy, which describes the interaction of nanotube with ground plane, using an atomic Lennard-Jones (L-J) potential. In the L-J potential, there are attractive and repulsive parts. The repulsive part decays very fast and plays an important role only when the nanotube is to contact with the ground. Since the major aim of this paper is to calculate the pull-in voltages, which leads to a deflection before contacting, it is reasonable to only consider the attractive part in the calculation of the van der Waals energy W using a pair-wise summation over all the atoms. As shown in figure 3, when a DWNT interacts with m layers of grapheme in the substrate, and if the interlayer distance of the grapheme is d, the van der Waals force of the DWNT can be written as [16]

$$f_2 = -\sum_{i=1}^{m} \left\{ \frac{\left[C_6\sigma_0^2\pi^2 r_1 \sqrt{g_i(g_i+2r_1)} \right](8g_i^4+32g_i^3r_1+72g_i^2r_1^2+80g_i r_1^3+35r_1^4)}{2g_i^5(g_i+2r_1)^5} + \right.$$
$$\left. \frac{\left[C_6\sigma_0^2\pi^2 r_0 \sqrt{g_i(g_i+2r_0)} \right](8g_i^4+32g_i^3r_0+72g_i^2r_0^2+80g_i r_0^3+35r_0^4)}{2g_i^5(g_i+2r_0)^5} \right\} \tag{16}$$

where r_0 and r_1 are the radii of the inner and outer nanotubes of the DWNT.

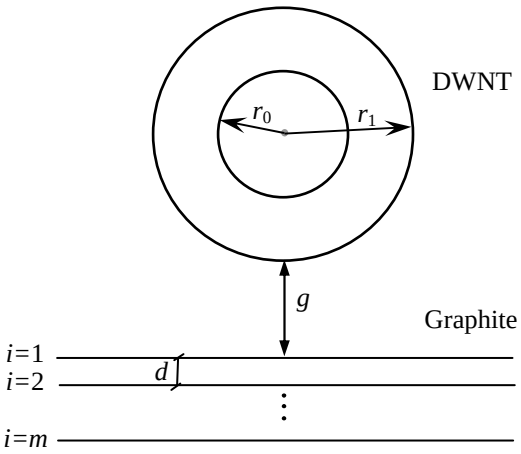

Fig. 3. A DWNT over a graphite ground plane

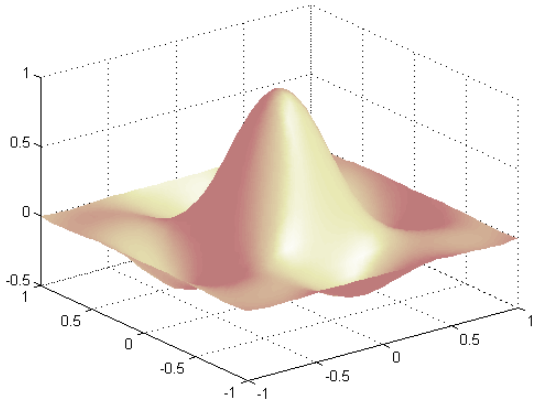

Fig. 4. The RBF meshfree shape function

Micro- and Nanotechnology: Materials, Processes, Packaging, and Systems IV
edited by Jung-Chih Chiao, Alex J. Hariz, David V. Thiel, Changyi Yang, Proc. of SPIE
Vol. 7269, 72690I · © 2008 SPIE · CCC code: 0277-786X/08/$18 · doi: 10.1117/12.813893

4. CONSTRUCTION OF RBF MESHFREE SHAPE FUNCTION

In equations (10) and (11), we need to construct the meshfree shape functions. At present, a number of ways to construct meshfree shape functions have been proposed. In this paper, the radial basis function (RBF) interpolation is used to construct the meshfree shape functions, because it is stable and accurate[7]. The locally supported RBF interpolation formulation can be written as:

$$u(\mathbf{x}) = \sum_{i=1}^{n} R_i(r) a_i + \sum_{j=1}^{m} p_j(\mathbf{x}) b_j = \mathbf{R}^T \mathbf{a} + \mathbf{B}^T \mathbf{b} = \{\mathbf{R} \quad \mathbf{B}\} \begin{Bmatrix} \mathbf{a} \\ \mathbf{b} \end{Bmatrix} \tag{17}$$

where $R_i(r)$ is the RBF, n is the number of nodes in the interpolation domain of point $\mathbf{x}$, $p_j(\mathbf{x})$ is monomials in the space coordinates $\mathbf{x}^T=[x,y]$, m is the number of polynomial basis functions, and coefficients a_i and b_j are interpolation constants. The unique variable in a RBF is the distance, r, between the interpolation point $\mathbf{x}$ and a field node $\mathbf{x}_i$, and it makes the RBF interpolation easily extend to three-dimensional problems.

There are a number of RBFs, and their characteristics in meshfree methods have been widely investigated [7]. In this paper, the following locally supported multi-quadrics (MQ) RBF is used to construct the meshfree shape function based on the local interpolation domains, which is written as

$$R_i(\mathbf{x}) = [r_i^2 + (\alpha_0 d_i)^2]^q \tag{18}$$

where α_0 is a dimensionless coefficient, and d_i is a parameter of the nodal spacing. The selections of two parameters (α_0 and q) will significantly influence the performance of MQ RBF. The effects of α_0 and q have been studied in details in many publications [7]. It has been found that α_0=1.0 and q=1.03 lead to good results for most problems in solids, and therefore, these values will be used in this paper.

Coefficients a_i and b_i in equation (17) can be solved by enforcing equation (17) to be satisfied at the n nodes surrounding a point $\mathbf{x}$. Then, Equation (17) can be re-written as the matrix form as follows

$$\begin{Bmatrix} \mathbf{u}_e \\ \mathbf{0} \end{Bmatrix} = \begin{bmatrix} \mathbf{R}_0 & \mathbf{B}_m \\ \mathbf{B}_m^T & \mathbf{0} \end{bmatrix} \begin{Bmatrix} \mathbf{a} \\ \mathbf{b} \end{Bmatrix} = \mathbf{G}\mathbf{a}_0 \tag{19}$$

where

$$\mathbf{B}_m^T = \begin{bmatrix} p_1(\mathbf{x}_1) & p_1(\mathbf{x}_2) & \cdots & p_1(\mathbf{x}_n) \\ p_2(\mathbf{x}_1) & p_2(\mathbf{x}_2) & \cdots & p_2(\mathbf{x}_n) \\ \vdots & \vdots & \ddots & \vdots \\ p_m(\mathbf{x}_1) & p_m(\mathbf{x}_2) & \cdots & p_m(\mathbf{x}_n) \end{bmatrix}, \quad \mathbf{R}_0 = \begin{bmatrix} R_1(r_1) & R_2(r_1) & \cdots & R_n(r_1) \\ R_1(r_2) & R_2(r_2) & \cdots & R_n(r_2) \\ \cdots & \cdots & \cdots & \cdots \\ R_1(r_n) & R_2(r_n) & \cdots & R_n(r_n) \end{bmatrix} \tag{20}$$

From equation (19), coefficients $\mathbf{a}_0$ can be solved and substituting $\mathbf{a}_0$ back into equation (17), the following RBF interpolation formulation is then obtained

$$u(\mathbf{x}) = \{\mathbf{R} \quad \mathbf{B}\}\mathbf{G}^{-1} \begin{Bmatrix} \mathbf{u}_e \\ \mathbf{0} \end{Bmatrix} = \{\mathbf{\Phi}(\mathbf{x}) \quad \mathbf{\Lambda}(\mathbf{x})\} \begin{Bmatrix} \mathbf{u}_e \\ \mathbf{0} \end{Bmatrix} \tag{21}$$

where the RBF shape function $\mathbf{\Phi}(\mathbf{x})$ is defined by

$$\mathbf{\Phi}(\mathbf{x}) = [\phi_1(\mathbf{x}), \phi_2(\mathbf{x}), ..., \phi_n(\mathbf{x})] = \left(\{\mathbf{R} \quad \mathbf{B}\}\mathbf{G}^{-1} \right)\Big|_{1-n} \tag{22}$$

where $\mathbf{\Phi}(\mathbf{x})$ is a vector which includes $1-n$ elements of $\{\mathbf{R} \quad \mathbf{B}\}\mathbf{G}^{-1}$. A sample of $\mathbf{\Phi}(\mathbf{x})$ is plotted in figure 4.

It has been proven that the RBF shape functions given in equation (22) satisfy the Kronecker delta condition, which makes it easy to enforce the boundary conditions in the meshfree method based on the RBF shape functions.

5. RESULTS AND DISCUSSIONS

A cantilever switch is considered to consist of a DWNT of 50 nm in length, with r_1 = 1 nm, and r_0 = 0.665 nm. The initial gap between the DWNT and the ground plane is 4 nm. There are 30 sheets of grapheme for the ground plane, and the inter-layer distance of graphite, d, is 0.335 nm, and $\varepsilon_0 = 8.854\times10^{-12}\,\mathrm{C^2N/m^2}$ [17].

Micro- and Nanotechnology: Materials, Processes, Packaging, and Systems IV
edited by Jung-Chih Chiao, Alex J. Hariz, David V. Thiel, Changyi Yang, Proc. of SPIE
Vol. 7269, 72690I · © 2008 SPIE · CCC code: 0277-786X/08/$18 · doi: 10.1117/12.813893

To analyze this switch, the MD is firstly used to extract the material parameters. The equivalent product of EI is obtained $7.58\times10^{-25}\mathrm{m}^2\mathrm{N}$. Then, the above meshfree formulation is used and 51 regularly distributed field nodes are employed to discretized this tube. It can be found that with the increase of the applied voltage, the deflection of the DWNT increases, and the gap between the tube and the ground plane decreases. When the voltage increases to a certain value, the tube becomes unstable suddenly and the free end of the tube will touch the bottom plane. This process is defined as the pull-in behavior [13] and the corresponding voltage value is called the critical pull-in voltage, at which the deflection of the tube tip equals to the initial gap. In the practical applications of nanoswitches, the critical pull-in voltage is one of the most important parameters.

Figure 5 demonstrates the result of the deflection of this DWNT tube tip under different voltages. It can be seen that the critical pull-in voltage is 0.47 volt. Compared with the same value, 0.5 volt, obtained by an analytical method [16][18] and other method [13], the presented method gives a very good result. It should be mentioned here that the above model is only valid when the tube deflection is small. Because of the decrease of the gap between the DWNT and the ground plane, both the electrostatic and van der Waals forces increase significantly, which pull the tube down suddenly. To simulate the deflection process after the critical pull-in voltage, a geometrically non-linear model must be developed.

Figure 6 demonstrates the relationship between the critical pull-in voltage and the initial gap for this switch. It clearly shows that the critical pull-in voltage increases with the increase of the initial gap. When the initial gap is larger than 6 nm, the slope for the curve changes very slowly, because with a large gap the effect of the van der Waals force is negligible. When the gap is very small, on the other hand, the van der Waals force will play a key role. At a critical gap value ($g \approx 3.5\mathrm{nm}$ in the present case), pull-in will occur even without an external voltage[13].

A fixed-fixed switch based on the same DWNT is also simulated. All computational parameters are the same as those listed above. The critical pull-in voltage is obtained now becomes 6.2 volt which is much higher than that of the cantilever switch. It is reasonable because a fixed-fixed tube is harder to be bended.

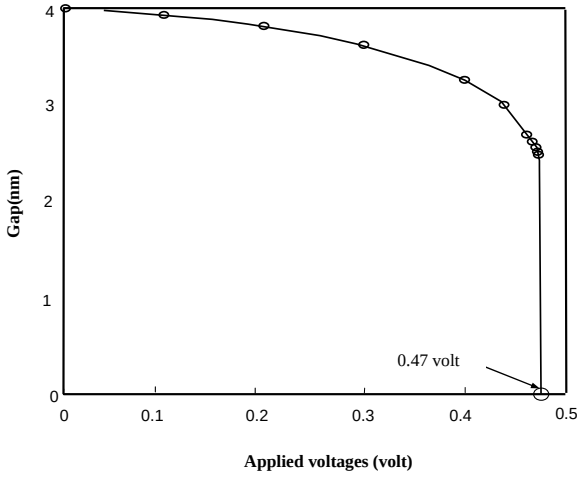

Fig. 5. The gap under different voltages for the cantilever DWNT based switch

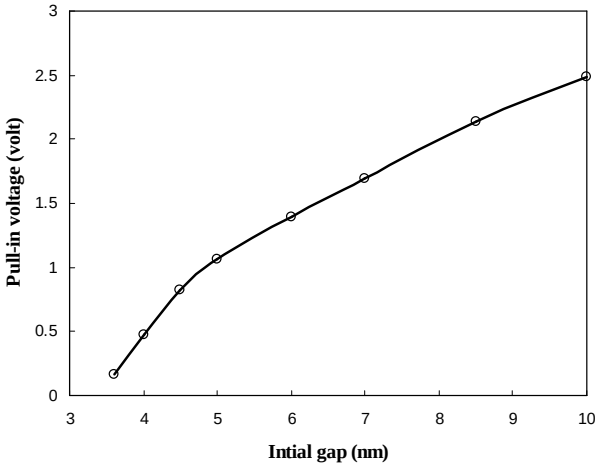

Fig. 6. Pull-in voltages vs. gaps for the cantilever DWNT based switch

6. CONCLUSION

This paper has developed an effective multiscale simulation technique for the deformation analysis of nanotube-based nanoswitches. The key material parameters, (e.g., Young's modulus and moment of inertia) are extracted from typical MD simulation which can explore the atomic properties. Then, the switches are simplified to continuum beam structure which is discretized and simulated by the advanced meshfree formulation. The pull-in voltage characteristics of nanoswitches based on the double-walled nanotube are studied. From studies of this paper, it has proven that the proposed technique is effective to give satisfactory deformation results for nanoswitches when the gap between the nanoswitch arm and the ground is not too small and not too big.

Micro- and Nanotechnology: Materials, Processes, Packaging, and Systems IV
edited by Jung-Chih Chiao, Alex J. Hariz, David V. Thiel, Changyi Yang, Proc. of SPIE
Vol. 7269, 72690I · © 2008 SPIE · CCC code: 0277-786X/08/$18 · doi: 10.1117/12.813893

ACKNOWLEDGEMENT

This work was supported by an ARC Discovery Grant.

REFERENCES

[1] Zhang L. and Tanaka H. (1999), "On the mechanics and physics in the nano-indentation of silicon mono-crystals", JSME International Journal, Series A: Solid Mechanics & Material Engineering 42, 546-559 (1999).
[2] Rapaport D.C., The Art of Molecular Dynamics Simulation. Cambridge University Press(1995).
[3] Abraham F., Broughton J., Bernstein N. and Kaxiras E., "Spanning the continuum to quantum length scales in a dynamic simulation of brittle fracture", Europhys. Lett. 44 (1998), 783–787.
[4] Broughton J.Q., Abraham F.F., Bernstein N. and Kaxiras E., "Concurrent coupling of length scales: methodology and application", Physical Review B, 60, 2391-2403 (1999).
[5] Gu Y.T. and Zhang L.C., "A concurrent multiscale method for structures based on the combination of the meshfree method and the molecular dynamics", Multiscale Modeling and Simulation 5 (4): 1128-1155(2006).
[6] Rudd R.E. and Broughton J.Q., "Coarse-grained molecular dynamics and the atomic limit of finite elements", Physical Review B, 58, 5893-5896(1998).
[7] Liu G.R. and Gu Y.T., An Introduction to Meshfree Methods and Their Programming. Springer, Berlin (2005).
[8] Liu G.R. and Gu Y.T. "A local radial point interpolation method (LR-PIM) for free vibration analyses of 2-D solids", Journal of Sound and Vibration, 246(1), 29-46(2001).
[9] Belytschko T., Lu Y.Y. and Gu L., "Element-Free Galerkin Methods", International Journal for Numerical Methods in Engineering, 37:229-256 (1994).
[10] Atluri S.N. and Zhu T., "A new meshless local Petrov-Galerkin (MLPG) approach in computational mechanics", Computational Mechanics, 22, 117-127 (1998)
[11] Gu Y.T. and Liu G.R., "A local point interpolation method for static and dynamic analysis of thin beams", Computer Method in Applied Mechacincs Engineering, 190, 5515-5528 (2001).
[12] Xiao S.P. and Belytschko T., "A bridging domain method for coupling continua with molecular dynamics", Computer Methods in Applied Mechanics and Engineering, 193, 1645-1669(2004).
[13] Gu Y.T. and Zhang L.C., "A simple method for analyzing the deformation of nanoelectromechanical switches based on carbon nanotubes", International Journal of Nano-Manufacturing, 1(2), 210-222 (2006).
[14] Zienkiewicz O.C. and Taylor R.L., The finite *element method* (5th ed.). Butterworth Heinemann, Oxford (2000).
[15] Vodenitcharova T. and Zhang L.C. "Effective wall thickness of a single-walled carbon nanotube", Physcial Review B, 68 165401(2003).
[16] Dequesnes M., Rotkin S.V. and Aluru N.R. "Calculation of pull-in voltages for carbon-nanotube-based nanoelectromechanical switches", Nanotechnology, 13 120–131 (2002).
[17] Jackson J.D., Classical Electrodynamics (3rd edn, Wiley, NewYork)(1998).
[18] Dequesnes M., Tang Z. and Aluru N.R.,"Static and Dynamic Analysis of Carbon Nanotube-Based Switches", J. of Engineering Materials and Technonoly, 126, 230-237 (2004).